Histochem Cell Biol
DOI 10.1007/s00418-009-0599-8

ORIGINAL PAPER

Localization of Nopp140 within mammalian cells during interphase and mitosis

Marc Thiry · Thierry Cheutin · Françoise Lamaye · Nicolas Thelen · U. Thomas Meier · Marie-Françoise O'Donohue · Dominique Ploton

Accepted: 31 March 2009

Abstract We investigated distribution of the nucleolar phosphoprotein Nopp140 within mammalian cells, using immunofluorescence confocal microscopy and immunoelectron microscopy. During interphase, three-dimensional image reconstructions of confocal sections revealed that nucleolar labelling appeared as several tiny spheres organized in necklaces. Moreover, after an immunogold labelling procedure, gold particles were detected not only over the dense fibrillar component but also over the fibrillar centres of nucleoli in untreated and actinomycin D-treated cells. Labelling was also consistently present in Cajal bodies. After pulse-chase experiments with BrUTP, colocalization was more prominent after a 10- to 15-min chase than after a 5-min chase. During mitosis, confocal analysis indicated that Nopp140 organization was lost. The protein dispersed between and around the chromosomes in prophase. From prometaphase to telophase, it was also detected in numerous cytoplasmic nucleolus-derived foci. During telophase, it reappeared in the reforming nucleoli of daughter nuclei. This strongly suggests that Nopp140 could be a component implicated in the early steps of pre-rRNA processing.

Keywords Nucleolus · Nopp140 · Confocal microscopy · Immunoelectron microscopy · Mitosis · Interphase · Mammalian cells

M. Thiry (✉) · F. Lamaye · N. Thelen
Laboratoire de Biologie Cellulaire et Tissulaire,
Université de Liège, 20 rue de Pitteurs, 4020 Liege, Belgium
e-mail: mthiry@ulg.ac.be

T. Cheutin · M.-F. O'Donohue · D. Ploton
UMRCNRS 6237, Université de Reims Champagne-Ardenne,
51 rue Cognacq-Jay, 51095 Reims Cedex, France

U. T. Meier
Department of Anatomy and Structural Biology,
Albert Einstein College of Medicine,
Bronx, New York, NY 10461, USA

Present Address:
T. Cheutin
Institut de Génétique Humaine CNRS,
141 rue de la Cardonille, 34396 Montpellier Cedex 5, France

Present Address:
M.-F. O'Donohue
Laboratoire de Biologie Moléculaire Eucaryote CNRS,
Université de Toulouse, 118 route de Narbonne,
31062 Toulouse Cedex 9, France

Introduction

The nucleolus is a prominent subnuclear compartment assembled around clusters of tandemly repeated rDNA genes, from which pre-RNAs are transcribed and subsequently modified, folded, processed and assembled into small and large ribosomal subunits (Thiry and Goessens 1996). Three morphologically distinct nucleolar components have been defined in interphase cells: the fibrillar centre (FC), the dense fibrillar component (DFC) and the granular component (GC). It is currently thought that each of these three components correlates with a specific step in ribosome biogenesis. During mitosis, in most eukaryotic cells, the nucleoli disappear at the end of prophase and reappear in daughter cells during telophase. Interestingly, several lines of evidence suggest that the mitotic fate of nucleolar components depends on their functional role in ribosome biogenesis (Dundr et al. 1997, 2000; Dundr and Olson 1998; Hernandez-Verdun and Gautier 1994; Scheer et al. 1993; Thiry and Goessens 1996). Indeed, the elements directly involved in rDNA transcription, such as RNA

Published online: 18 April 2009

polymerase I (Pol I), upstream binding factor (UBF) or DNA topoisomerase I, although inactive from prophase until early telophase, remain mainly associated with the nucleolus organizer region (NOR) throughout the different steps of mitosis (Chan et al. 1991; Guldner et al. 1986; Jordan et al. 1996; Roussel et al. 1996; Scheer and Rose 1984; Sirri et al. 1999; Weisenberger and Scheer 1995). On the contrary, components involved in pre-rRNA processing are concentrated in the perichromosomal sheath or in nucleolus-derived foci (NDFs). They are re-utilized throughout telophase in the formation of new nucleoli through different prenucleolar bodies (PNBs, Dundr et al. 1997, 2000; Dundr and Olson 1998; Fomproix and Hernandez-Verdun 1999; Hernandez-Verdun and Gautier 1994; Jimenez-Garcia et al. 1994; Savino et al. 1999, 2001; Verheggen et al. 2000; Weisenberger and Scheer 1995).

The present study focussed on the nonribosomal, nucleolar protein, Nopp140 (Meier and Blobel 1990). Originally isolated from rat (Meier and Blobel 1990, 1992), this protein was later identified in human (Pai et al. 1995), *Xenopus* (Cairns and McStay 1995), yeast (Meier 1996), *Drosophila* (Waggener and DiMario 2002) and trypanosomes (Kelly et al. 2006). Unlike most other nucleolar proteins, Nopp140 does not carry RNA-binding motifs or glycine/arginine-rich stretches, as deduced from the known primary sequences of different species. On the contrary, its amino- and carboxy-termini are separated by a long, central domain, consisting of ten repeats of acidic serine clusters alternating with lysine-, alanine- and proline-rich basic stretches. Most serine residues of the acidic repeats are phosphorylated by casein kinase 2, which makes Nopp140 one of the most highly phosphorylated proteins in the cell with ~80 phosphates per molecule (Li et al. 1997; Meier and Blobel 1992; Meier 1996). Despite these biochemical characteristics, the biological functions of Nopp140 are still unclear. Interaction of Nopp140 with p80-coilin, a constituent of the Cajal body (CB, Andrade et al. 1991), suggests that Nopp140 functions as a molecular link between the nucleolus and the CBs (Isaac et al. 1998). A mammalian nucleolar protein, NAP57, has also been identified as a Nopp140-associated protein, found in the DFC of the nucleolus and in the CBs (Meier and Blobel 1994). Possible roles for NAP57 were mostly deduced from analysis of its yeast homologue, Cbf5p, characterized as a putative rRNA pseudouridine synthase involved in rRNA synthesis and pre-rRNA processing (Cadwell et al. 1997; Lafontaine et al. 1998). In addition, Nopp140 associates with the two major classes of small nucleolar ribonucleoprotein particles (snoRNPs, Yang et al. 2000) which mainly catalyse rRNA modification (Lafontaine and Tollervey 1998). Thus, Nopp140 could function as a chaperone for the biogenesis and transport of snoRNPs (Isaac et al. 1998; Meier 2005; Yang et al. 2000). However, unlike components implicated in pre-rRNA processing, Nopp140 is not associated with the NDFs and with the PNBs during mitosis (Dundr et al. 1997). On the other hand, Nopp140 was found to interact with the largest subunit of Pol I, suggesting a role in rDNA transcription (Chen et al. 1999). However, unlike the transcriptional machinery of Pol I, Nopp140 does not associate with the mitotic NORs (Dundr et al. 1997; Pai et al. 1995; Schmidt-Zachmann et al. 1984; Tsai et al. 2008). Intriguingly, it has been shown previously that Nopp140 functions as Pol II transcription coactivator, and interacts with the general transcription factor TFIIB and a specific DNA motif-binding transcription factor (Miau et al. 1997). However, the localization of Nopp140 in the nucleolus and the CBs strongly suggests its involvement in cellular activities carried out within these structures.

In order to shed light on the cellular function of Nopp140, the present study re-investigated the precise location of this protein within different mammalian cells during the cell cycle by immunofluorescence confocal microscopy coupled to three-dimensional (3D) image reconstructions and immunogold electron microscopy. The results revealed that Nopp140 was detected in the CBs and in the nucleoli. In the latter case, the labelling of the FC and the surrounding DFC was organised in tiny spheres. These were rapidly associated with ribosomal RNA transcripts as revealed by pulse-chase experiments. During mitosis, Nopp140 was not a NOR-associated protein, but it was dispersed in numerous NDFs. The functional significance of these findings is discussed.

Materials and methods

Biological materials

HeLa cells and HEp-2 cells were grown at 37°C under 5% CO_2 in Glasgow minimum essential medium (Life Technologies, Gent, Belgium) supplemented with 10% fetal calf serum. Ehrlich ascites tumour cells (ELT) were grown in a medium composed of 40% NCTC 109, 40% Hanks solution, 20% fetal calf serum, 100 U/ml penicillin. Some cultures of ELT cells were treated for 1–2 h with 0.05 or 20 µg/ml actinomycin D (Sigma, St Louis, USA).

Immunofluorescence methods

The slides were simultaneously fixed and permeabilized for 4 min at room temperature in 4% formaldehyde and 1% (vol/vol) Triton X-100 in 0.1 M PBS (pH 7.4). After washing in PBS containing 1% BSA (w/v) and normal goat serum (NGS) diluted 1/30, they were placed for 30 min at 37°C with anti-Nopp140 polyclonal antibodies (RF12 and RE10; Meier and Blobel 1992) diluted 1/200 in PBS,

containing NGS diluted 1/50 and 0.2% BSA. After rinsing with PBS containing 1% BSA, the slides were incubated for 30 min at 37°C with FITC-conjugated goat anti-rabbit antibody (Sigma) diluted 1/100 in PBS containing 0.2% BSA. After rinsing, the slides were mounted with Citifluor™ AF1 (Agar Scientific, Stansted, UK).

For double-labelling experiments, the slides were fixed for 5 min at room temperature in 4% formaldehyde in 0.1 M PBS (pH 7.4) containing 1% Triton X-100. They were rinsed in PBS, and then in PBS containing 1% BSA, as well as NGS and normal sheep serum (NSS), diluted 1/30. They were incubated for 30 min at 37°C with anti-Nopp140 polyclonal antibodies diluted 1/200 in PBS, containing 0.2% BSA and NGS diluted 1/50. The slides were washed with PBS containing 1% BSA and incubated for 30 min at 37°C with an FITC-conjugated goat anti-rabbit antibody diluted 1/100 in PBS containing 0.2% BSA. After rinsing, the slides were incubated for 30 min at 37°C with rabbit anti-CHO nucleolin serum (kindly provided by Dr F. Amalric) diluted 1/200 in PBS, containing 0.2% BSA and NSS, diluted 1/50. The slides were washed with PBS containing 1% BSA and incubated for 30 min at 37°C with a biotinylated sheep anti-rabbit antibody (Roche Diagnostics) diluted 1/100 in PBS containing 0.2% BSA. This secondary antibody was detected with streptavidin labelled with Texas Red (Amersham Life Science, Little Chalfont, UK) diluted 1/100 in PBS containing 0.2% BSA for 10 min. After rinsing, the slides were mounted with Citifluor AF1.

Pulse-chase experiments were carried out as previously described by Thiry et al. (2000, 2008).

Confocal microscopy and three-dimensional visualisations

A Biorad 1024ES system (Bio-Rad, Hercules, CA, USA), mounted on an inverted IX70 Olympus optical microscope, was used. Acquisitions, made using a planapochromat 60×, 1.4 numerical aperture oil immersion objective, were performed by exciting the FITC with the 488-nm line of a Krypton/Argon laser. The emission light was collected through a band-pass filter at 522 ± 16 nm. Phase contrast images were collected simultaneously on a specific detector. For 3D investigations, 30–50 optical sections were recorded from the top of the cell with a 0.5-µm z-step and reconstructed as described (Heliot et al. 1997; Klein et al. 1998). Surfacic visualization was then applied (Cheutin et al. 2002; Klein et al. 1998).

Immunoelectron microscopy

Culture, permeabilization, incorporation and washings were all carried out at room temperature, in Petri dishes. Cells were fixed for 60–90 min in 4% formaldehyde in 0.1 M Sörensen's buffer (pH 7.4). After fixation, the cells were washed in Sorensen's buffer, dehydrated through graded ethanol solutions and then processed for embedding in Lowicryl K4M according to the technique of Roth et al. (1981). The immunolabellings were performed as previously described (Vandelaer and Thiry 1998). For immunolabelling, several primary antibodies were used: anti-Nopp140 polyclonal antibodies (diluted 1/200), anti-CHO and human nucleolin serum (diluted 1/200) from rabbit (kindly provided by Dr F. Amalric), anti-B36 Mab P2G3 (diluted 1/20; Christensen et al. 1986; kindly provided by Dr F. Puvion-Dutilleul) and anti-p80 coilin polyclonal antibody (diluted 1/100) from rabbit (Carmo-Fonseca et al. 1992; kindly provided by Dr R. Deltour). Two control experiments were carried out, in which either the primary antibodies were omitted, or the sections were incubated with antibody-free gold particles. The ultrathin sections were stained with uranyl acetate and lead citrate before examination in a Jeol CX 100 II electron microscope at 60 kV.

Quantitative evaluations

Since the electron-dense marker used in the immunogold technique is particulate, the density of labelling can be quantified. As demonstrated previously, only antigenic sites exposed at the surface of the sections can interact with the antibodies (Bendayan 1984). Therefore, the labelling density is independent of the section thickness but is directly related to the areas occupied by each of the intracellular compartments. Since differences in observed labelling densities reflect relative differences in the concentration of antigenic sites, only relative comparisons between intensities can be considered. To evaluate the labelling density, the area of each compartment (Sa) was estimated using a morphometrical approach by the point-counting method (Weibel 1969). Then, the number of gold particles (Ni) present over each compartment was counted and the labelling density (Ns) calculated (Ns = Ni/Sa). Values obtained on the resin and the cytoplasm can be considered as background staining.

Results

Localization of Nopp140 during interphase

In order to analyse the intracellular location of Nopp140, an indirect immunofluorescence method was applied on HeLa cells, simultaneously fixed with formaldehyde and permeabilized with Triton X100. After probing Nopp140 either with a polyclonal antibody (RF12) more specific for rodents or a polyclonal antibody (RE10) more specific for primates, the labelling was analysed by confocal microscopy. Similar results were obtained in both cases. Comparison

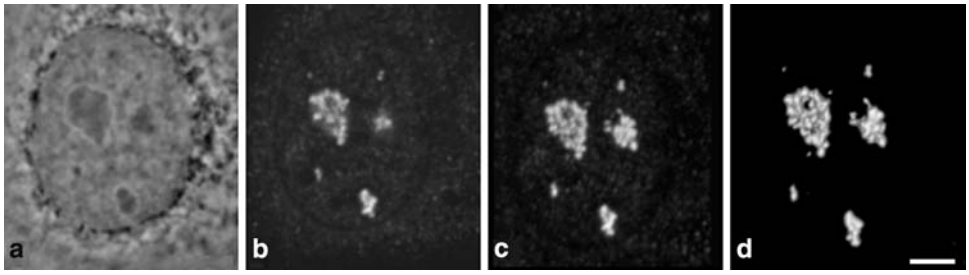

Fig. 1 Distribution of Nopp140 in a HeLa cell during interphase observed by confocal microscopy. **a** Phase contrast, **b** optical section, **c** projection of the z-series, **d** surfacic visualisation of the volume. Results show a strong labelling localized in the cell nucleoli and in the nuclear Cajal bodies. As revealed by 3D reconstructions, the nucleolar labelling is organized as *spherical spots* grouped in clusters (**c, d**). Bar is 5 µm

between a phase contrast image (Fig. 1a) and a single optical section (Fig. 1b) showed that Nopp140 labelling was found in most parts of the nucleoli. In addition, the labelling was observed in extranucleolar dots, which are reminiscent of Cajal bodies, as observed for cells stained with anti-p80 coilin antibodies (Meier and Blobel 1994). In the control experiments, no label was seen when anti-Nopp140 antibodies were replaced by preimmune serum. The 3D distribution of Nopp140 was obtained by volume reconstruction from the stack (z-series) of confocal optical sections, visualized either as a projection (Fig. 1c), or as a volume with surfacic rendering mode (Fig. 1d). Nopp140 labelling was seen as multiple fluorescent spots that were grouped in clusters (Fig. 1b, c). The fluorescent spots are individual beads, 0.5 µm in diameter, which are organized as a necklace (Fig. 1d).

To localize precisely Nopp140 with regard to the nucleolar ultrastructural components, immunoelectron microscopy experiments were performed on ultrathin sections of Lowicryl K4M-embedded HeLa, ELT and HEp-2 cells. The results were similar with all three cell types and both antibodies to Nopp140. Gold particles were clearly evidenced over the DFC and the FC, notably in the peripheral region of this compartment (Fig. 2a, b). On the contrary, both the GC and the condensed chromatin were completely devoid of labelling. These observations were confirmed after quantification of the labelling density over the different cellular compartments in three different cell types (Table 1). Indeed, the labelling density was very high over the DFCs, but it was still significant over the FCs. By contrast, the labelling density was very low over the GC, and its value was not significant in the nucleoplasm. The distribution of fibrillarin and nucleolin in three cell types was investigated using specific antibodies revealed by gold particles. The electron micrographs showed that anti-B36 antibodies, directed against fibrillarin, preferentially labelled the DFC (Fig. 2c), whereas anti-nucleolin antibodies strongly marked the GC and the DFC (Fig. 2d). However, in both cases, no labelling was observed over the FCs.

The nucleolar distribution of Nopp140 was also studied in cells treated with actinomycin D. This transcriptional inhibitor induces a complete reorganization of the nucleolar ultrastructural compartments, whose disposition with respect to the condensed chromatin becomes polarized. As observed in previous studies (Thiry and Goessens 1996), the order of succession is always as follows: condensed chromatin–FC–DFC–GC. When cells were submitted to actinomycin D, Nopp140 was located in both fibrillar components (DFC and FC) of segregated nucleoli (Fig. 3a). In contrast, no label was present over the GC. In the same experimental conditions, fibrillarin was detected in the DFC of segregated nucleoli (Fig. 3b), and nucleolin was seen both over the GC and the DFC (Fig. 3c). In both cases, the FCs were totally devoid of gold particles.

Finally, immunoelectron microscopy experiments were performed on ultrathin sections of HeLa, ELT and HEp-2 cells in order to determine whether the extranucleolar labelling observed with anti-Nopp140 antibodies corresponded to CBs (Fig. 4). An antibody directed against p80 coilin, a specific marker of CBs, unambiguously confirmed that this nuclear compartment was similar to that revealed with the Nopp140 probes (data not shown). After quantification, the labelling density over the CBs was comparable to that obtained over the DFC of the nucleolus (Table 1).

Having localized Nopp140, we attempted to determine whether this location corresponds to a particular stage in the formation of pre-rRNAs within the nucleolus. To perform this study, the spatial distribution of pre-rRNAs (Fig. 5, green) obtained in HeLa cells lipofected with BrUTP for increasing times of chase was compared to that of Nopp140 (Fig. 5, red) on single optical sections. After short chase periods, the relative surface of colocalization of the two signals in the nucleoli was low. BrUTP labelling was detected as round spots at the centre of nucleoli, whereas the Nopp140 labelling occupied a wider zone (Fig. 5a–c). Colocalization of Nopp140 and BrUTP was assessed with MetaMorph software. A scatter-plot was used to select the pixels which displayed high levels of both

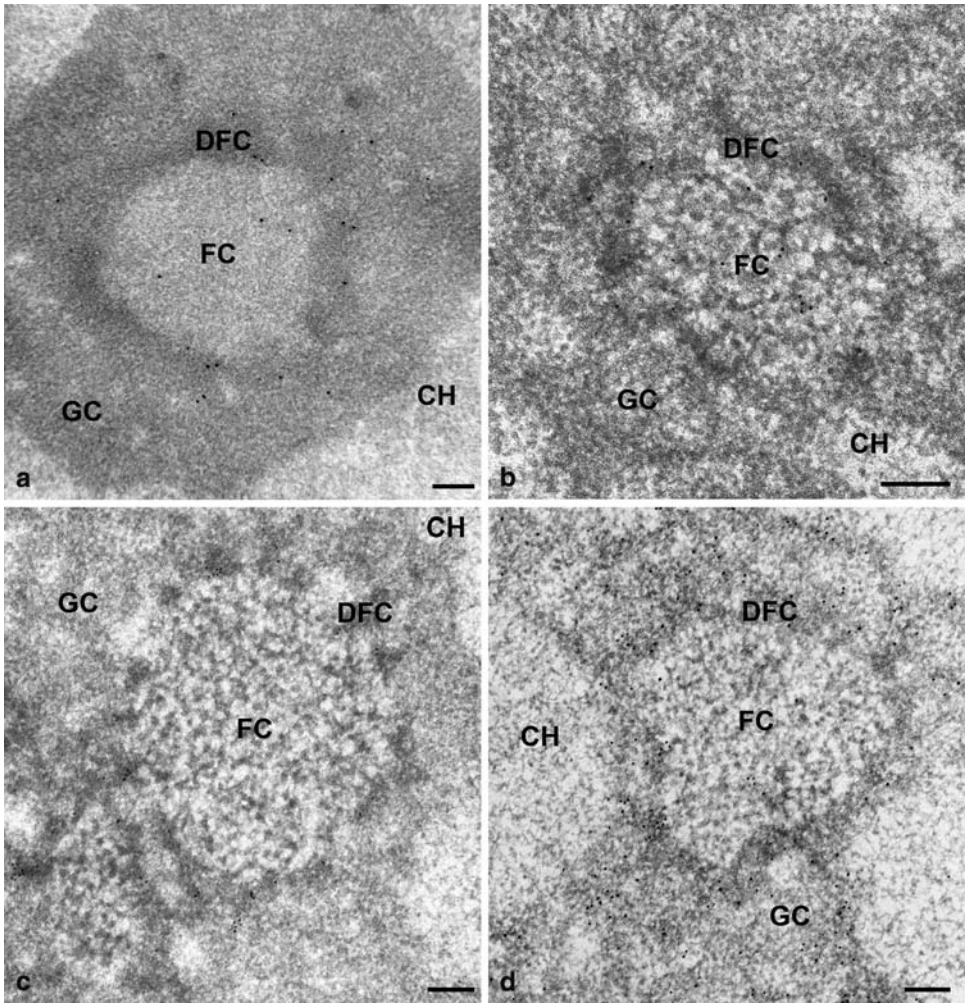

Fig. 2 Immunoelectron microscopy localization of Nopp140, fibrillarin and nucleolin within the nucleolus. Ultrathin sections of HeLa (**a**) and ELT (**b–d**) cells were immunolabelled with specific anti-serum RE10 (**a**) and anti-serum RF12 (**b**), corresponding to anti-Nopp140 antibodies, and with antibodies directed against fibrillarin (**c**) and nucleolin (**d**). **a, b** Gold particles are located over the fibrillar centres (FC) and the dense fibrillar component (DFC), while the granular component (GC) is devoid of label. **c** The DFC is labelled by anti-fibrillarin antibodies. The FCs and the GC are not labelled. **d** Both the FCs and the GC are strongly labelled by anti-nucleolin antibodies, while the FCs are devoid of labelling. *CH* condensed chromatin. Bars are 0.2 µm

Table 1 Gold particle densities (number of particles per square micrometre) over the different structural compartments in HeLa, ELT and HEp-2 cells after immunogold labelling using anti-Nopp140 antibodies (RE10 or RF12); 552, 654, 633 and 228 gold particles were counted, respectively

	Mean values ± SEM			
	HeLa cells	ELT cells		HEp-2 cells
	RE10, $n = 12$	RF12, $n = 19$	RE10, $n = 12$	RE10, $n = 9$
Nucleus				
Nucleolus				
Fibrillar centres	5.36 ± 1.33*	5.72 ± 2.30*	6.64 ± 2.53*	7.36 ± 2.25*
Dense fibrillar component	18.45 ± 5.30*	20.33 ± 7.18*	22.59 ± 4.32*	23.79 ± 5.95*
Granular component	1.63 ± 0.91	1.40 ± 0.52	1.40 ± 0.51	2.52 ± 0.94
Nucleoplasm[a]	1.01 ± 0.13	0.54 ± 0.19	0.48 ± 0.14	0.36 ± 0.22
Cajal bodies		18.12 ± 5.45*		17.11 ± 5.74*
Cytoplasm	0.62 ± 0.49			0.55 ± 0.31
Resin		0.92 ± 0.12	0.80 ± 0.27	

Student's *t*-test for cellular compartments vs. resin or cytoplasm (*$P < 0.01$)

[a] Condensed chromatin included

green and red, thus corresponding to colocalizing species. As quantified from Fig. 5a, b, 65.3% of Nopp140 labelling overlapped with the BrUTP signal within the nucleoli after 5-min incorporation. Fifteen minutes after transfection (Fig. 5d, e), quantification revealed that 89.3% of Nopp140 colocalized with the nucleolar transcripts. Indeed, BrRNAs

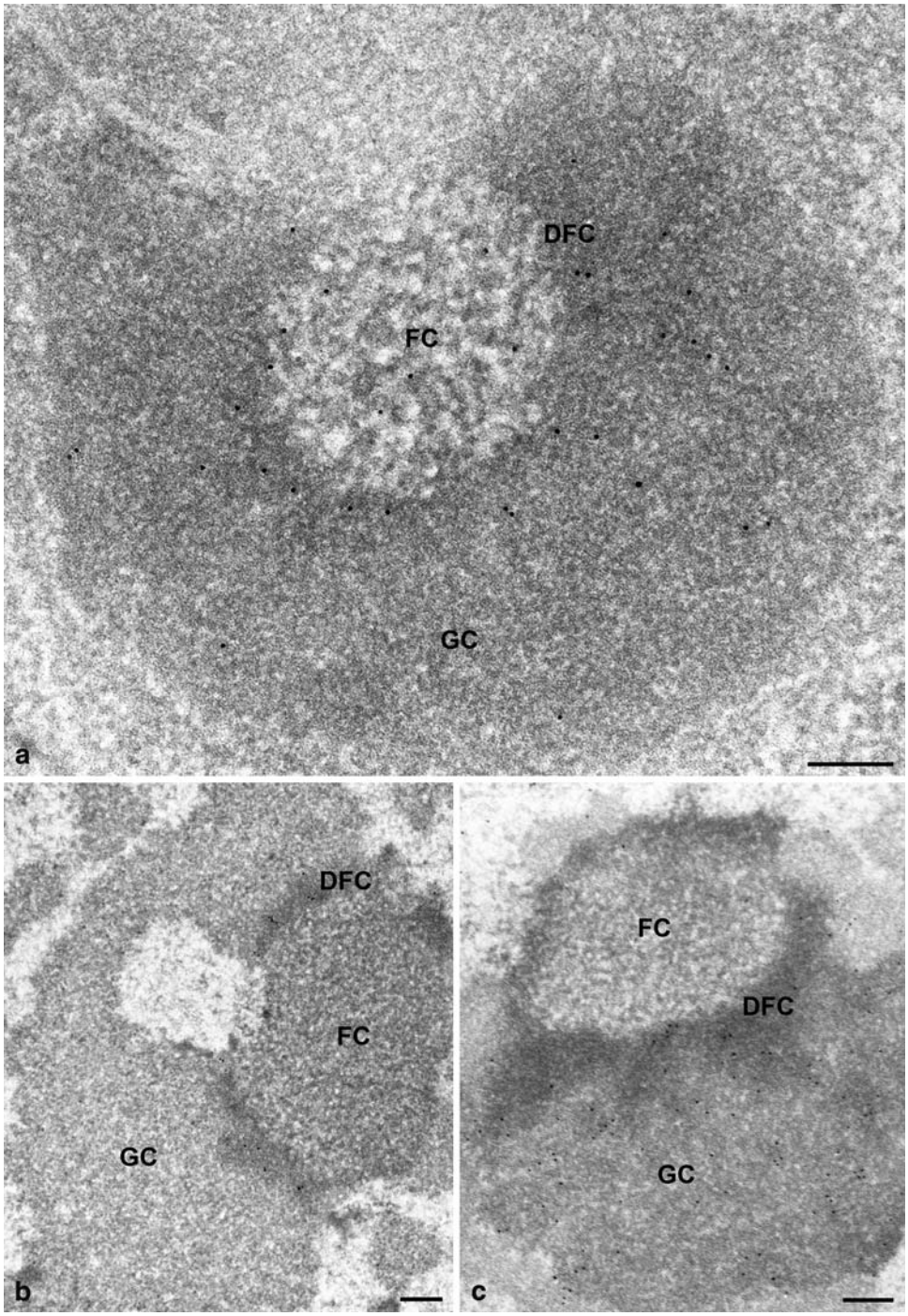

Fig. 3 Immunoelectron microscopy localization of Nopp140 (**a**), fibrillarin (**b**) and nucleolin (**c**) within the nucleolus in cells treated with actinomycin D. Ultrathin sections of ELT cells, treated for 2 h with 0.05 µg/ml actinomycin D, were immunolabelled with anti-Nopp140 (RE10) (**a**), anti-fibrillarin (**b**) and anti-nucleolin (**c**) antibodies. **a** In the segregated nucleolus, labelling was clearly evidenced over the FCs and the DFC, while the GC displayed only a few rare gold particles. **b** The DFC of the segregated nucleolus is the only compartment labelled by anti-fibrillarin antibodies. No labelling was observed over the FCs and the GC. **c** Both the DFC and the GC were labelled by anti-nucleolin antibodies, while the FC was devoid of particles. Bars are 0.2 µm

and Nopp140 displayed almost identical patterns in the nucleoli, as seen on the overlay (Fig. 5f).

Fate of Nopp140 throughout mitosis

Nopp140 labelling was analysed in HeLa cells by confocal microscopy during the various steps of mitosis, after an indirect immunofluorescence labelling procedure. During prophase, Nopp140 was associated with disintegrated nucleoli (Fig. 6a–f). The labelling was less structured than during interphase and consisted of several large spots and many fine fluorescent foci. It progressively dispersed in the nucleoplasm between the chromosomes (Fig. 6c) and after the breakdown of the nuclear envelope became cytoplasmic (Fig. 6e, f). In metaphase (Fig. 6g, h), the labelling was totally disorganized. However, it seemed preferentially located in the perichromosomal regions on both sides of the metaphase plate (Fig. 6g). Although most labelling was diffuse, brighter spots were also evidenced. Clearly, NORs were not stained by anti-Nopp140 antibodies, in contrast to

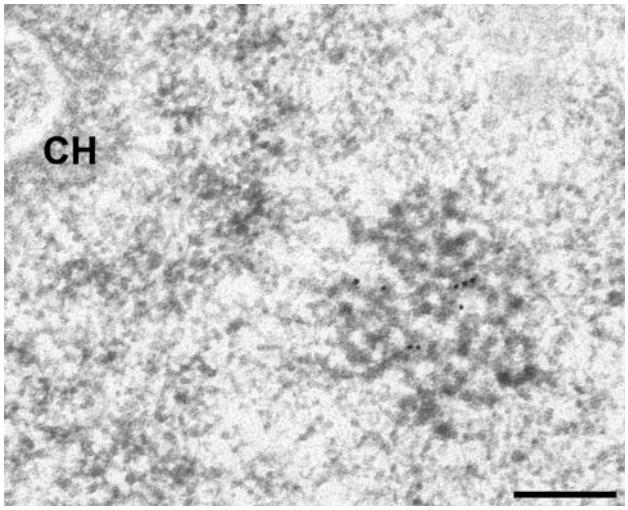

Fig. 4 Immunoelectron microscopy localization of Nopp140 in extranucleolar regions of cell nuclei. The micrograph displays a Cajal body of a HEp-2 cell in which Nopp140 is detected. *CH* condensed chromatin. Bar is 0.05 µm

what was observed with antibodies directed against Pol I (Heliot et al. 1997), UBF (Klein et al. 1998) or pp135 (Weisenberger and Scheer 1995). In anaphase (Fig. 6i, j), the labelling was homogeneously distributed throughout the cytoplasm, but brighter spots were also detected between the separating chromosomes (Fig. 6i). During telophase (Fig. 7a–t), Nopp140 labelling was clearly cytoplasmic, as it was mainly seen around the reforming daughter nuclei (Fig. 7b–k). However, a few faint nuclear spots were seen in mid-telophase (Fig. 7e–l). In later stages of telophase, the intensity of these spots progressively increased (Fig. 7m–p). The presence of Nopp140 in the cytoplasm of cells during telophase was clearly evidenced by using a double labelling with nucleolin, a marker of NDFs (Fig. 8).

Discussion

This study revealed that the nonribosomal protein Nopp140 is located in nucleoli and CBs of mammalian cells during interphase and is associated with the NDFs during mitosis.

Its behaviour during mitosis is similar to that of proteins involved in pre-rRNA processing. Indeed, we showed that Nopp140, like components implicated in pre-rRNA processing, including U3 snoRNA, fibrillarin, nucleolin and proteins B23 and p52, accumulates in perichromosomal regions and in numerous NDFs between prometaphase and late telophase (DiMario 2004; Dundr et al. 1997; Dundr

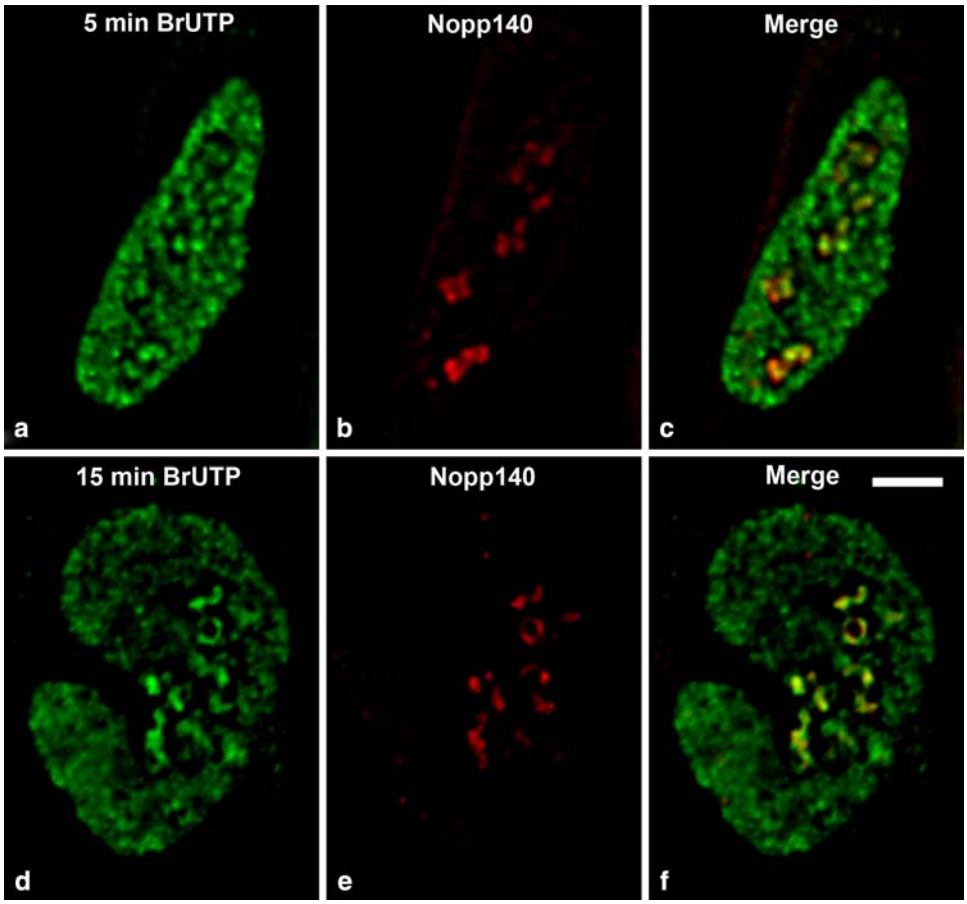

Fig. 5 Time-dependent migration of BrUTP-rRNAs in comparison with Nopp140-positive sites within the nucleolus. Double immunofluorescence detection of BrUTP-labelled rRNAs (*green*, **a, d**) and Nopp140 (*red*, **b, e**) in HeLa cells cultured in medium without BrUTP for 5 min (**a–c**) and 15 min (**d–f**) after lipofection with BrUTP-FuGene-6 complexes and observed on single optical sections. Overlay of *green* and *red signals* (**c, f**). Bar is 5 µm

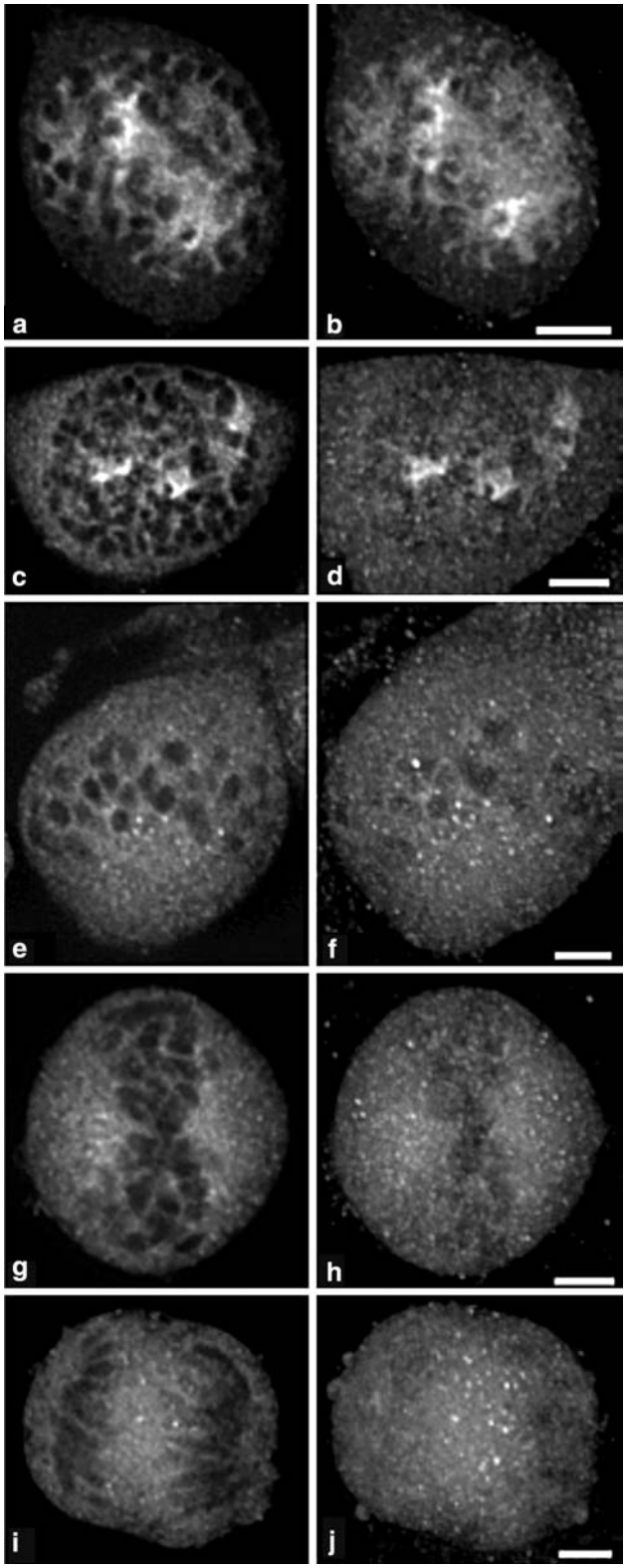

Fig. 6 Confocal microscopy analyses of Nopp140 distribution in HeLa cells from prophase to anaphase. Single optical sections (**a, c, e, g, i**) and projections of the corresponding z-series (**b, d, f, h, j**) show Nopp140 distribution during the first steps of mitosis. **a–d** Early prophase, **e–f** late prophase, **g–h** metaphase, **i–j** anaphase. Bars are 5 μm

and Olson 1998; Hernandez-Verdun and Gautier 1994). However, using double-immunofluorescence labelling of specific NDF markers, Dundr et al. (1997) concluded that Nopp140 was not associated with the NDFs from anaphase to telophase in different types of mammalian cells. These structures could be different from those previously reported. In previous immunofluorescence experiments, p130, the human homologue of Nopp140, appeared to be located in granular structures, resembling the PNBs at telophase (Pai et al. 1995). Similar observations were obtained with the *Xenopus* homologue of the rat nucleolar protein Nopp140, xNopp180 (Schmidt-Zachmann et al. 1984). These data already suggest that Nopp140 could belong to components involved in pre-rRNA processing. More recently, it has been demonstrated that Nopp140 interacts with both classes of snoRNPs, required for rRNA modification and processing, and that it functions as a chaperone for their biogenesis and intranuclear transport (Isaac et al. 1998; Yang et al. 2000). In agreement with our ultrastructural localizations of Nopp140, snoRNAs have been detected preferentially in the DFC of nucleoli. By in situ hybridization at the electron microscope level, U3 snoRNA has been visualised essentially in the DFC (Puvion-Dutilleul et al. 1991). This RNA catalyses the initial processing of the 5′ external transcribed spacer and also the subsequent processing events around the 18S region (Hughes 1996; Kass et al. 1990; Savino and Gerbi 1990). Other snoRNAs, such as MRP and U8, which catalyse respectively the processing within internal transcribed spacer I, and at the 5.8S and 28S borders (Chu et al. 1994; Peculis and Steitz 1993; Schmitt and Clayton 1993), have also been located in the DFC or in a subregion thereof (Jacobson et al. 1995; Matera et al. 1994; Reimer et al. 1988).

Our 3D reconstruction through interphase cells clearly indicates that the Nopp140 labelling appears as beads organized in necklaces in the nucleolar volume. Moreover, we showed that Nopp140 is present in the DFC of nucleoli, as previously reported (Meier and Blobel 1992), but is also seen in the FCs. This discrepancy probably arises from differences in fixation procedures. Indeed, we noticed that the presence of 0.1% glutaraldehyde in the fixation buffer abolishes the labelling in both fibrillar components of nucleoli. In the first assay for locating Nopp140 at the ultrastructural level, 0.05% glutaraldehyde was employed in the fixation solution, and a clear labelling was only found in the DFC. Interestingly, this nucleolar distribution coincides with the 3D and ultrastructural location of pre-rRNAs as observed after a short pulse with BrUTP (the present study and Thiry et al. 2000). In previous double immunofluorescence labelling experiments, it has been further demonstrated that Nopp140 colocalized with Pol I in the nucleolus (Baran et al. 2001; Chen et al. 1999; Tsai et al. 2008). However, contrary to proteins involved in rDNA transcription

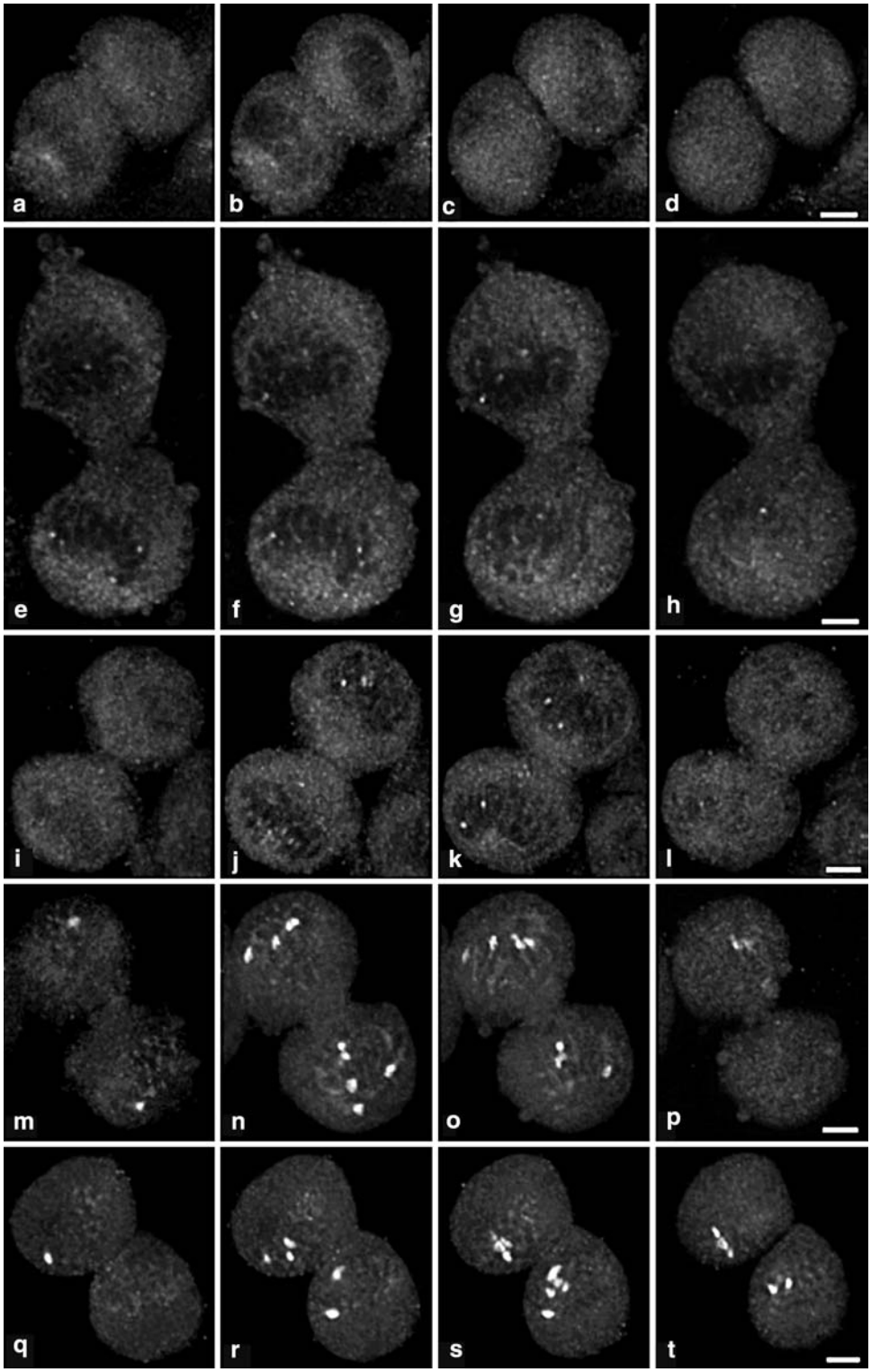

Fig. 7 Confocal microscopy analyses of Nopp140 distribution in HeLa cells during telophase. **a–d** Selection of four optical sections of z-series displaying a cell in early telophase. **e–h, i–l** Selection of four optical sections of z-series displaying a cell in mid-telophase. **m–p** Selection of four optical sections of z-series displaying a cell in late telophase. **q–t** Selection of four optical sections of z-series displaying a cell at the beginning of G1. Bars are 5 μm

such as Pol I, UBF, DNA topoisomerase I, TATA-binding protein (TBP), TBP-associated proteins and transcription terminator factor TTF-1 (Chan et al. 1991; Guldner et al. 1986; Jordan et al. 1996; Roussel et al. 1996; Scheer and Rose 1984; Sirri et al. 1999; Weisenberger and Scheer 1995), our results also show that Nopp140 is not associated with the NORs throughout mitosis. These results indicate that Nopp140 is not an element of Pol I transcriptional machinery, even though it is located in the vicinity of the rDNA sites during transcription, which have been shown to be located in the FCs in previous reports (Cheutin et al. 2002; Derenzini et al. 2006). Interestingly, it has been

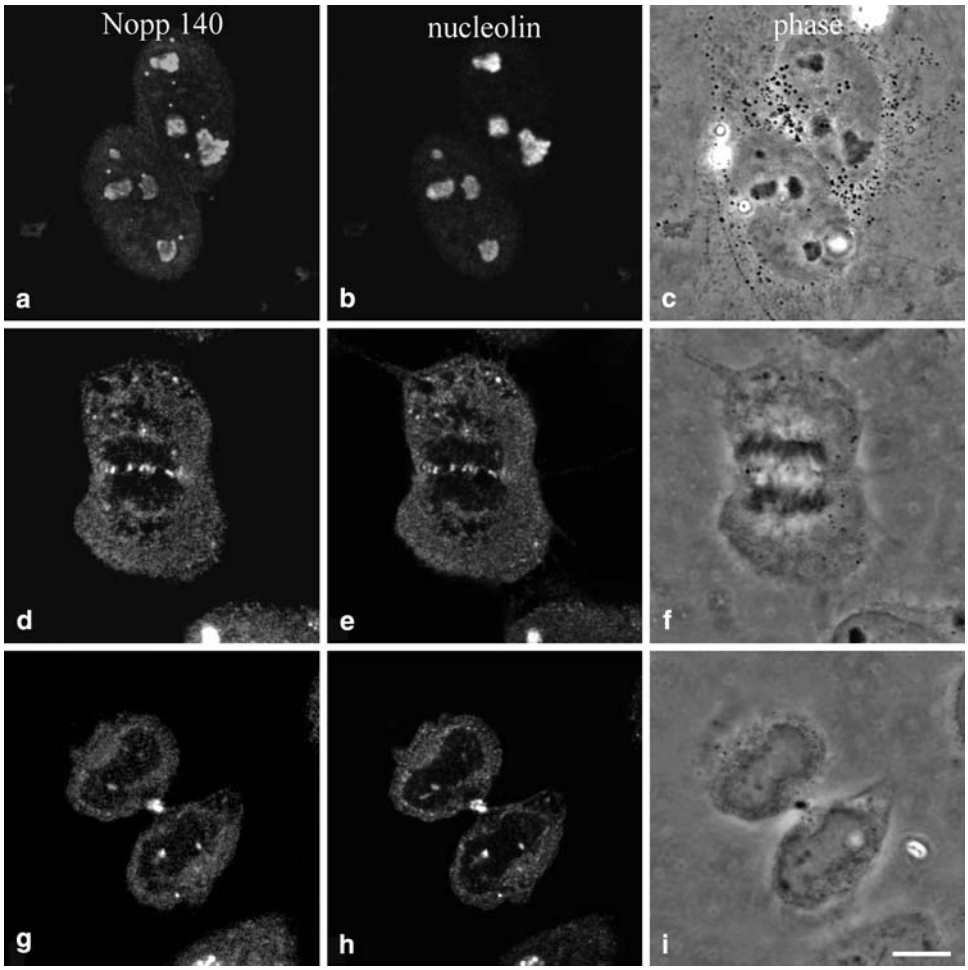

Fig. 8 Confocal microscopy analyses (one optical section) of Nopp140 and nucleolin distribution in HeLa cells during interphase (**a–c**), anaphase (**d–f**), end of telophase (**g–i**). Bar is 5 μm

shown that Pol I transcription was arrested in nucleoli depleted of snoRNPs, raising the possibility of a feedback mechanism between rRNA modification and transcription (Yang et al. 2000). All these data suggest that Nopp140 should be a component implicated in pre-rRNA processing at the rDNA transcription active sites.

Contrary to previous immunogold labelling assays, we observed never curvilinear tracks that extended for microns across the nucleoplasm from the DFC of the nucleolus to the nuclear pore complexes. However, such tracks have never been visualised in immunofluorescence preparations and our ultrastructural results are entirely consistent with the previous immunofluorescence observations (Meier and Blobel 1992, 1994). Indeed, the only nuclear structures to be labelled outside the nucleolus are the CBs. In the present study, we also showed the labelling distribution at the ultrastructural level. The presence of Nopp140 in CBs supports the view that these nuclear structures are involved in nucleolar functions (Isaac et al. 1998; Meier and Blobel 1994; Verheggen et al. 2001a, b). Their content in different snRNAs suggests that CBs may play a general role in the cell such as import, assembly and storage of components implicated in different steps of both nucleolar and extranucleolar RNA metabolism.

Acknowledgments The authors wish to thank Drs F. Amalric, R. Deltour and F. Puvion-Dutilleul for their generous gift of antibodies. They also acknowledge the skillful technical provided by F. Skivée and D. Bourguignon. This work received financial support from the "Fonds de la Recherche Scientifique Médicale" (grant no. 3. 3.4540.06) to M. Thiry, from the "Ligue Régionale de la Marne", from the "Fondation pour la Recherche Médicale" (grant no. 40001837–01) to D. Ploton, and from the National Institute of Health (HL079566) to U.T. Meier, F. Lamaye and N. Thelen are Ph.D. grant holders of the F.N.R.S.

References

Andrade LE, Chan EK, Raska I, Peebles CL, Roos G, Tan EM (1991) Human autoantibody to a novel protein of the nuclear coiled body: immunological characterization and cDNA cloning of p80-coilin. J Exp Med 173:1407–1419

Baran V, Brochard V, Renard JP, Flechon JE (2001) Nopp 140 involvement in nucleologenesis of mouse preimplantation embryos. Mol Reprod Dev 59:277–284

Bendayan M (1984) Protein A-gold electron microscopic immunocytochemistry: methods, applications and limitations. J Electron Microsc Tech 1:243–270

Cadwell C, Yoon HJ, Zebarjadian Y, Carbon J (1997) The yeast nucleolar protein Cbf5p is involved in rRNA biosynthesis and interacts genetically with the RNA polymerase I transcription factor RRN3. Mol Cell Biol 17:6175–6183

Cairns C, McStay B (1995) Identification and cDNA cloning of a *Xenopus* nucleolar phosphoprotein, xNopp180, that is the homolog of the rat nucleolar protein Nopp140. J Cell Sci 108:3339–3347

Carmo-Fonseca M, Pepperkok R, Carvalho MT, Lamond AI (1992) Transcription-dependent colocalization of the U1, U2, U4/U6, and U5 snRNPs in coiled bodies. J Cell Biol 117:1–14

Chan EK, Imai H, Hamel JC, Tan EM (1991) Human autoantibody to RNA polymerase I transcription factor hUBF. Molecular identity of nucleolus organizer region autoantigen NOR-90 and ribosomal RNA transcription upstream binding factor. J Exp Med 174:1239–1244

Chen HK, Pai CY, Huang JY, Yeh NH (1999) Human Nopp140, which interacts with RNA polymerase I: implications for rRNA gene transcription and nucleolar structural organization. Mol Cell Biol 19:8536–8546

Cheutin T, O'Donohue MF, Beorchia A, Vandelaer M, Kaplan H, Deféver B, Ploton D, Thiry M (2002) Three-dimensional organization of active rRNA genes within the nucleolus. J Cell Sci 115:3297–3307

Christensen ME, Moloo J, Swischuk JL, Schelling ME (1986) Characterization of the nucleolar protein, B-36, using monoclonal antibodies. Exp Cell Res 166:77–93

Chu S, Archer RH, Zengel JM, Lindahl L (1994) The RNA of RNase MRP is required for normal processing of ribosomal RNA. Proc Natl Acad Sci USA 91:659–663

Derenzini M, Pasquinelli G, O'Donohue MF, Ploton D, Thiry M (2006) Structural and functional organization of ribosomal genes within the mammalian cell nucleolus. J Histochem Cytochem 54:131–145

DiMario P (2004) Cell and molecular biology of nucleolar assembly and disassembly. Int Rev Cytol 239:99–178

Dundr M, Olson MO (1998) Partially processed pre-rRNA is preserved in association with processing components in nucleolus-derived foci during mitosis. Mol Biol Cell 9:2407–2422

Dundr M, Meier UT, Lewis N, Rekosh D, Hammarskjold ML, Olson MO (1997) A class of nonribosomal nucleolar components is located in chromosome periphery and in nucleolus-derived foci during anaphase and telophase. Chromosoma 105:407–417

Dundr M, Misteli T, Olson MO (2000) The dynamics of postmitotic reassembly of the nucleolus. J Cell Biol 150:433–446

Fomproix N, Hernandez-Verdun D (1999) Effects of anti-PM-Scl 100 (Rrp6p exonuclease) antibodies on prenucleolar body dynamics at the end of mitosis. Exp Cell Res 251:452–464

Guldner HH, Szostecki C, Vosberg HP, Lakomek HJ, Penner E, Bautz FA (1986) Scl 70 autoantibodies from scleroderma patients recognize a 95 kDa protein identified as DNA topoisomerase I. Chromosoma 94:132–138

Heliot L, Kaplan H, Lucas L, Klein C, Beorchia A, Doco-Fenzy M, Menager M, Thiry M, O'Donohue MF, Ploton D (1997) Electron tomography of metaphase nucleolar organizer regions: evidence for a twisted-loop organization. Mol Biol Cell 8:2199–2216

Hernandez-Verdun D, Gautier T (1994) The chromosome periphery during mitosis. Bioessays 16:179–185

Hughes JM (1996) Functional base-pairing interaction between highly conserved elements of U3 small nucleolar RNA and the small ribosomal subunit RNA. J Mol Biol 259:645–654

Isaac C, Yang Y, Meier UT (1998) Nopp140 functions as a molecular link between the nucleolus and the coiled bodies. J Cell Biol 142:319–329

Jacobson MR, Cao LG, Wang YL, Pederson T (1995) Dynamic localization of RNase MRP RNA in the nucleolus observed by fluorescent RNA cytochemistry in living cells. J Cell Biol 131:1649–1658

Jimenez-Garcia LF, Segura-Valdez ML, Ochs R, Rothblum LI, Hanwan R, Spector DL (1994) Nucleologenesis: U3 snRNA-containing prenucleolar bodies move to sites of active pre-rRNA transcription after mitosis. Mol Biol Cell 5:955–966

Jordan P, Mannervik M, Tora L, Carmo-Fonseca M (1996) In vivo evidence that TATA-binding protein/SL1 colocalizes with UBF and RNA polymerase I when rRNA synthesis is either active or inactive. J Cell Biol 133:225–234

Kass S, Tyc K, Steitz JA, Sollner-Webb B (1990) The U3 small nucleolar ribonucleoprotein functions in the first step of preribosomal RNA processing. Cell 60:897–908

Kelly S, Singleton W, Wickstead B, Ersfeld K, Gull K (2006) Characterization and differential nuclear localization of Nopp140 and a novel Nopp140-like protein in trypanosomes. Eukaryotic Cell 5:876–879

Klein C, Cheutin T, O'Donohue MF, Rothblum L, Kaplan H, Beorchia A, Lucas L, Heliot L, Ploton D (1998) The three-dimensional study of chromosomes and upstream binding factor-immunolabeled nucleolar organizer regions demonstrates their nonrandom spatial arrangement during mitosis. Mol Biol Cell 9:3147–3159

Lafontaine DL, Tollervey D (1998) Birth of the snoRNPs: the evolution of the modification-guide snoRNAs. Trends Biochem Sci 23:383–388

Lafontaine DL, Bousquet-Antonelli C, Henry Y, Caizergues-Ferrer M, Tollervey D (1998) The box H + ACA snoRNAs carry Cbf5p, the putative rRNA pseudouridine synthase. Genes Dev 12:527–537

Li D, Meier UT, Dobrowolska G, Krebs EG (1997) Specific interaction between casein kinase 2 and the nucleolar protein Nopp140. J Biol Chem 272:3773–3779

Matera AG, Tycowski KT, Steitz JA, Ward DC (1994) Organization of small nucleolar ribonucleoproteins (snoRNPs) by fluorescence in situ hybridization and immunocytochemistry. Mol Biol Cell 5:1289–1299

Meier UT (1996) Comparison of the rat nucleolar protein nopp140 with its yeast homolog SRP40. Differential phosphorylation in vertebrates and yeast. J Biol Chem 271:19376–19384

Meier UT (2005) The many facets of H/ACA ribonucleoproteins. Chromosoma 114:1–14

Meier UT, Blobel G (1990) A nuclear localization signal binding protein in the nucleolus. J Cell Biol 111:2235–2245

Meier UT, Blobel G (1992) Nopp140 shuttles on tracks between nucleolus and cytoplasm. Cell 70:127–138

Meier UT, Blobel G (1994) NAP57, a mammalian nucleolar protein with a putative homolog in yeast and bacteria. J Cell Biol 127:1505–1514

Miau LH, Chang CJ, Tsai WH, Lee SC (1997) Identification and characterization of a nucleolar phosphoprotein, Nopp140, as a transcription factor. Mol Cell Biol 17:230–239

Pai CY, Chen HK, Sheu HL, Yeh NH (1995) Cell-cycle-dependent alterations of a highly phosphorylated nucleolar protein p130 are associated with nucleologenesis. J Cell Sci 108:1911–1920

Peculis BA, Steitz JA (1993) Disruption of U8 nucleolar snRNA inhibits 5.8S and 28S rRNA processing in the *Xenopus* oocyte. Cell 73:1233–1245

Puvion-Dutilleul F, Mazan S, Nicoloso M, Christensen ME, Bachellerie JP (1991) Localization of U3 RNA molecules in nucleoli of HeLa and mouse 3T3 cells by high resolution in situ hybridization. Eur J Cell Biol 56:178–186

Reimer G, Raska I, Scheer U, Tan EM (1988) Immunolocalization of 7–2-ribonucleoprotein in the granular component of the nucleolus. Exp Cell Res 176:117–128

Roth J, Bendayan M, Carlemalm E, Villiger W, Garavito M (1981) Enhancement of structural preservation and immunocytochemical staining in low temperature embedded pancreatic tissue. J Histochem Cytochem 29:663–671

Roussel P, André C, Comai L, Hernandez-Verdun D (1996) The rDNA transcription machinery is assembled during mitosis in active NORs and absent in inactive NORs. J Cell Biol 133:235–246

Savino R, Gerbi SA (1990) In vivo disruption of *Xenopus* U3 snRNA affects ribosomal RNA processing. EMBO J 9:2299–2308

Savino TM, Bastos R, Jansen E, Hernandez-Verdun D (1999) The nucleolar antigen Nop52, the human homologue of the yeast ribosomal RNA processing RRP1, is recruited at late stages of nucleologenesis. J Cell Sci 112:1889–1900

Savino TM, Gebrane-Younes J, De Mey J, Sibarita JB, Hernandez-Verdun D (2001) Nucleolar assembly of the rRNA processing machinery in living cells. J Cell Biol 153:1097–1110

Scheer U, Rose K (1984) Localization of RNA polymerase I in interphase cells and mitotic chromosomes by light and electron microscopic immunocytochemistry. Proc Natl Acad Sci USA 81:1431–1435

Scheer U, Thiry M, Goessens G (1993) Structure, function and assembly of the nucleolus. Trends Cell Biol 3:236–241

Schmidt-Zachmann MS, Hugle B, Scheer U, Franke WW (1984) Identification and localization of a novel nucleolar protein of high molecular weight by a monoclonal antibody. Exp Cell Res 153:327–346

Schmitt M, Clayton D (1993) Nuclear RNase MRP is required for correct processing of pre-5.8S in *Saccharomyces cerevisiae*. Mol Cell Biol 13:7935–7941

Sirri V, Roussel P, Hernandez-Verdun D (1999) The mitotically phosphorylated form of the transcription termination factor TTF-1 is associated with the repressed rDNA transcription machinery. J Cell Sci 112:3259–3268

Thiry M, Goessens G (1996) The nucleolus during the cell cycle. RG Landes Company/Chapman & Hall, New York

Thiry M, Cheutin T, O'Donohue MF, Kaplan H, Ploton D (2000) Dynamics and three-dimensional localization of ribosomal RNA within the nucleolus. RNA 6:1750–1761

Thiry M, Lamaye F, Thelen N, Chatron-Colliet A, Lalun N, Bobichon H, Ploton D (2008) A protocol for studying the kinetics of RNA within cultured cells: application to ribosomal RNA. Nat Protoc 3:1997–2004

Tsai Y-T, Lin C-I, Chen H-K, Lee K-M, Hsu C-Y, Yang S-J, Yeh N-H (2008) Chromatin tethering effects of hNopp140 are involved in the spatial organization of the nucleolus and the rRNA gene transcription. J Biomed Sci 15:471–486

Vandelaer M, Thiry M (1998) The phosphoprotein pp135 is an essential constituent of the fibrillar components of nucleoli and of coiled bodies. Histochem Cell Biol 110:169–177

Verheggen C, Almouzni G, Hernandez-Verdun D (2000) The ribosomal RNA processing machinery is recruited to the nucleolar domain before RNA polymerase I during *Xenopus laevis* development. J Cell Biol 149:293–306

Verheggen C, Le Panse S, Almouzni G, Hernandez-Verdun D (2001a) Maintenance of nucleolar machineries and pre-rRNAs in remnant nucleolus of erythrocyte nuclei and remodeling in *Xenopus* egg extracts. Exp Cell Res 269:23–34

Verheggen C, Mouaikel J, Thiry M, Blanchard JM, Tollervey D, Bordonne R, Lafontaine DL, Bertrand E (2001b) Box C/D small nucleolar RNA trafficking involves small nucleolar RNP proteins, nucleolar factors and a novel nuclear domain. EMBO J 20:5480–5490

Waggener JM, DiMario PJ (2002) Two splice variants of Nopp140 in *Drosophila melanogaster*. Mol Biol Cell 13:362–381

Weibel E (1969) Stereological principles for morphometry in electron microscopic cytology. Int Rev Cytol 26:235–302

Weisenberger D, Scheer U (1995) A possible mechanism for the inhibition of ribosomal RNA gene transcription during mitosis. J Cell Biol 129:561–575

Yang Y, Isaac C, Wang C, Dragon F, Pogacic V, Meier UT (2000) Conserved composition of mammalian box H/ACA and box C/D small nucleolar ribonucleoprotein particles and their interaction with the common factor Nopp140. Mol Biol Cell 11:567–577